Available online at www.sciencedirect.com
ScienceDirect
Journal of Power Sources 163 (2007) 943–951
JOURNAL OF POWER SOURCES
www.elsevier.com/locate/jpowsour

Catalytic steam reforming of methane, methanol, and ethanol over Ni/YSZ: The possible use of these fuels in internal reforming SOFC

N. Laosiripojana [a,*], S. Assabumrungrat [b]

[a] *The Joint Graduate School of Energy and Environment, King Mongkut's University of Technology Thonburi, Bangkok 10140, Thailand*
[b] *Center of Excellence on Catalysis and Catalytic Reaction Engineering, Department of Chemical Engineering, Chulalongkorn University, Bangkok 10330, Thailand*

Received 6 September 2006; received in revised form 1 October 2006; accepted 3 October 2006
Available online 13 November 2006

Abstract

This study investigated the possible use of methane, methanol, and ethanol with steam as a direct feed to Ni/YSZ anode of a direct internal reforming Solid Oxide Fuel Cell (DIR-SOFC). It was found that methane with appropriate steam content can be directly fed to Ni/YSZ anode without the problem of carbon formation, while methanol can also be introduced at a temperature as high as 1000 °C. In contrast, ethanol cannot be used as the direct fuel for DIR-SOFC operation even at high steam content and high operating temperature due to the easy degradation of Ni/YSZ by carbon deposition. From the steam reforming of ethanol over Ni/YSZ, significant amounts of ethane and ethylene were present in the product gas due to the incomplete reforming of ethanol. These formations are the major reason for the high rate of carbon formation as these components act as very strong promoters for carbon formation.

It was further observed that ethanol with steam can be used for an indirect internal reforming operation (IIR-SOFC) instead. When ethanol was first reformed by Ni/Ce–ZrO_2 at the temperature above 850 °C, the product gas can be fed to Ni/YSZ without the problem of carbon formation. Finally, it was also proposed from the present work that methanol with steam can be efficiently fed to Ni/YSZ anode (as DIR operation) at the temperature between 900 and 975 °C without the problem of carbon formation when SOFC system has sufficient space volume at the entrance of the anode chamber, where methanol can homogeneously convert to CH_4, CO, CO_2, and H_2 before reaching SOFC anode.

Keywords: Internal reforming; Ethanol; Methanol; Methane; SOFC

1. Introduction

Solid Oxide Fuel cell (SOFC) is an electrochemical energy conversion unit that converts chemical energy to electrical energy and heat with greater energy efficiency and lower pollutant emission than combustion process [1]. This type of fuel cell is expected to apply in power applications, i.e. for power plant (300 MWel) or as combined heat and power generation [1,2]. SOFC is also being investigated for using as an auxiliary power unit (APU) in mobile applications and as a portable system [1].

It is well established that hydrogen and carbon monoxide can be typically used as the fuels for SOFC. Furthermore, as SOFC is generally operated at such a high temperature (700–1100 °C), it is known that some hydrocarbons (i.e. methane) can also be directly used as fuels instead of hydrogen and carbon monoxide by feeding straight to the anode side of SOFC; this operation is called a direct internal reforming SOFC (DIR-SOFC). According to this operation, the hydrocarbon fuels are reformed at the anode producing hydrogen and carbon monoxide, which are electrochemically consumed for generating electricity simultaneously. The advantage of DIR-SOFC is that the hydrogen consumption by the electrochemical reaction could directly promote the reforming or conversion of hydrocarbons at the anode side. Therefore, DIR-SOFC results in high conversion and high efficiency [3].

DIR-SOFC operation requires an anode material that has good catalytic reforming and electrochemical reactivities. Ni/YSZ is the most common SOFC anode material due to its cost

* Corresponding author. Tel.: +66 2 8729014; fax: +66 2 8726736.
E-mail address: navadol_l@jgsee.kmutt.ac.th (N. Laosiripojana).

0378-7753/$ – see front matter © 2006 Elsevier B.V. All rights reserved.
doi:10.1016/j.jpowsour.2006.10.006

effective compared with other supported metals (e.g., Co, Pt, Ru, and Rh) and also well fitting with fuel cell design requirements. In addition, this material also provides catalytic reforming activity, which is beneficial for the DIR-SOFC operation. The nickel content for Ni/YSZ anode is usually 40–60% in order to match the thermal expansion of YSZ [4]. Some previous researchers have investigated the performance of DIR-SOFC operation fueled by methane. Yentekakis et al. [5] investigated the effect of steam on methane steam reforming rate over nickel–yttria stabilized zirconia cermets (Ni/YSZ) in the temperature range from 800 to 930 °C by varying the ratio of H_2O/CH_4 from 0.15 to 2.0. The experiment indicated the strong influence of steam on the reforming rate, which could be due to the steam deficiency. In contrast, Achenbach and Riensche [6] reported no influence of inlet steam partial pressure on the methane steam reforming rate over nickel cermet (20 wt% Ni and 80 wt% ZrO_2) at 700–940 °C with the inlet H_2O/CH_4 ratio from 2.6 to 8.0. Dicks et al. [7] observed that the dependence of methane steam reforming rate over Ni/ZrO_2 anode was a function of both temperature and gas compositions. They also reported that the steam reforming of methane over nickel/zirconia exhibited non-Arrhenius behavior in the temperature range of 700–1000 °C. It should be noted that most of the previous works on DIR-SOFC have concluded that the major difficulty of DIR-SOFC operation over Ni/YSZ is the possible formation of carbon species on the surface of Ni due to cracking of hydrocarbons. This formation could obstruct gas access and degrade anode performance by blocking the catalyst active sites resulting in the loss of cell performance and poor durability.

Another alternative internal reforming operation is an indirect internal reforming (IIR-SOFC). By this operation, the reforming reaction takes place at the reformer, which is in close thermal contact with the anode side of SOFC. IIR-SOFC gives the advantage of good heat transfer between the reformer and the fuel cell and is expected to provide an autothermal operation. In addition, unlike DIR-SOFC, the reformer part and the anode side for IIR-SOFC operation are operated separately. Therefore, the catalyst for reforming reaction at the reformer part and the material for electrochemical reactions at the anode side of fuel cell can be optimized individually preventing the possible degradation of anode from the carbon deposition.

Focusing on the fuel selection, currently, methane is the major fuel for SOFC due to its well developed and cost effective. Nevertheless, the use of alcohols (i.e. methanol and ethanol) should be also possible when operated as an internal or in-stack reforming. Methanol is favorable due to its ready availability, high-specific energy and storage transportation convenience [8,9], while ethanol is also a promising candidate, since it is readily produced from renewable resources (e.g., fermentation of biomasses) and has reasonably high hydrogen content [10,11]. Douvartzides et al. [12] applied a thermodynamic analysis to evaluate the feasibility of different fuels, i.e. methane, methanol, and ethanol for SOFC. The results obtained in terms of electromotive force output and efficiency show that ethanol and methanol are very promising alternatives to hydrogen.

In the present work, the first approach was to study the possible uses of alcohols (i.e. methanol and ethanol) as the fuels for DIR-SOFC by feeding these fuels as well as steam over Ni/YSZ. The reforming activity as well as the effects of fuel type, the fuel/steam ratio, and operating temperature on the degradation of Ni/YSZ by carbon deposition were determined. It should be noted that methane was also used as the feed in the present work for comparison. Secondly, in order to study the possible use of these fuels for IIR-SOFC operation, an annular ceramic reactor was designed and constructed. Details of this reactor configuration will be described in Section 2.1. Each fuel (i.e. methane, methanol, and ethanol) was fed into this annular reactor together with steam at several operating conditions, and the degradation of Ni/YSZ by carbon deposition was then investigated. Finally, the suitable operation (DIR or IIR) and conditions (the fuel/steam ratio, and operating temperature) of each fuel for SOFC were then determined.

2. Experimental

2.1. Annular reactor configuration

An annular ceramic reactor was constructed in order to study the use of hydrocarbon fuels for IIR operation (Fig. 1). According to the design, the reforming catalyst ($Ni/Ce–ZrO_2$) was packed at the inner side of the annular reactor, where the inlet gas was firstly introduced. At the end of the inner tube, all gas components flowed backward through the outer side of this annular reactor, where 300 mg of Ni/YSZ (with SiC) was packed. Therefore, both $Ni/Ce–ZrO_2$ and Ni/YSZ are operated at the same operating temperature. The main obligation of $Ni/Ce–ZrO_2$ is to reform all hydrocarbons before reaching the surface of Ni/YSZ preventing the degradation of Ni/YSZ by the carbon formation. It should be noted that $Ni/Ce–ZrO_2$ was selected as the reforming catalyst because the excellent reforming reactivity of this catalyst was reported recently [13].

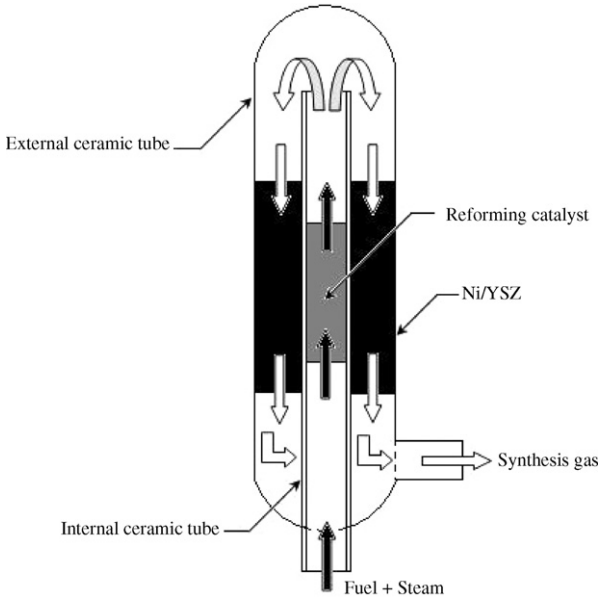

Fig. 1. Configuration of annular ceramic reactor for experiments under IIR operation.

2.2. Material preparation and characterization

$Ce_{0.75}Zr_{0.25}O_2$ support was prepared by co-precipitation of cerium nitrate ($Ce(NO_3)_3{\cdot}H_2O$), and zirconium oxychloride ($ZrOCl_2{\cdot}H_2O$) (from Aldrich). The molar ratio of ([Ce])/[cetyltrimethylammonium bromide] was kept constant at 0.8. It should be noted that aqueous solution of 0.1 M cetyltrimethylammonium bromide solution (from Aldrich), was also added in the cerium nitrate and zirconium oxychloride solution as a cationic surfactant. Our previous work reported that the preparation of ceria-based material by this surfactant-assisted method can achieve the high surface area and high thermal stability material due to the incorporation of surfactants during preparation, which reduces the interfacial energy and eventually decreases the surface tension of water contained in the pores [14–16]. The starting solution was prepared by mixing 0.1 M of metal salt solution with 0.4 M of urea at a 2 to 1 volumetric ratio. This solution was stirred by magnetic stirring (100 rpm) for 3 h, and the precipitate was filtered and washed with deionised water and ethanol to prevent an agglomeration of the particles. It was dried overnight in an oven at 110 °C, and then calcined in air at 1000 °C for 6 h. Ni/Ce–ZrO_2 was prepared by impregnating above Ce–ZrO_2 with $Ni(NO_3)_2$ solution (from Aldrich), whereas Ni/YSZ was prepared by mixing NiO (42.86 vol%) with YSZ (57.14 vol%) with a ball milling for 18 h at room temperature. These catalysts were calcined in air at 1000 °C for 6 h and then reduced with 10% H_2/Ar for 6 h before use.

After reduction, the catalysts were characterized with several physicochemical methods. The weight content of Ni in Ni/Ce–ZrO_2 and Ni/YSZ was determined by X-ray fluorescence (XRF) analysis. The reducibility and dispersion percentages of nickel were measured from temperature-programmed reduction (TPR) with 5% H_2 in Ar and temperature-programmed desorption (TPD), respectively. All physicochemical properties of the synthesized catalysts are presented in Table 1.

2.3. Apparatus and procedures

An experimental reactor system was constructed as shown elsewhere [13–16]. The feed gases including the components of interest (ethanol, methanol, methane, and steam) and the carrier gas (helium) were introduced to the reaction section, in which either a quartz reactor (for DIR studying) or the annular ceramic reactor (for IIR studying) was mounted vertically inside a furnace. Ni/YSZ (with SiC) was loaded in the quartz reactor, which was packed with a small amount of quartz wool to prevent the catalyst from moving. In the case of the annular reactor, Ni/Ce–ZrO_2 and Ni/YSZ were packed inside the reactor as described in Section 2.1. Regarding the results in our previous publications [13–16], to avoid any limitations by intraparticle diffusion, the constant residence time of 5×10^{-4} g min cm^{-3} was applied in all experiments. A Type-K thermocouple was placed into the annular space between the reactor and the furnace. This thermocouple was mounted on the tubular reactor in close contact with the catalyst bed to minimize the temperature difference between the catalyst bed and the thermocouple. Another Type-K thermocouple was inserted in the middle of the quartz tube in order to re-check the possible temperature gradient. The record showed that the maximum temperature fluctuation during the reaction was always ±0.75 °C or less from the temperature specified for the reaction. After the reactions, the exit gas mixture was transferred via trace-heated lines to the analysis section, which consisted of a Porapak Q column Shimadzu 14B gas chromatograph (GC) and a mass spectrometer (MS).

Table 1
Physicochemical properties of the catalysts after reduction

Catalyst	Ni-load[a] (wt%)	Ni-reducibility[b] (Ni%)	Ni-dispersion[c] (Ni%)
Ni/Ce–ZrO_2	4.8	92.4	4.74
Ni/YSZ	39	95.9	

[a] Measured from X-ray fluorescence analysis.
[b] Measured from temperature-programmed reduction (TPR) with 5% hydrogen.
[c] Measured from temperature-programmed desorption (TPD) of hydrogen after TPR measurement.

The effects of temperature, type of fuel, and inlet fuel/steam molar ratios on the amount of carbon formation over catalysts and the product distribution from the steam reforming reaction were studied. In order to study the formation of carbon species on catalyst surface, temperature-programmed oxidation (TPO) was applied by introducing 10% oxygen in helium, after the catalyst was purged with helium. The operating temperature was increased from 100 to 1000 °C at a rate of 20 °C min^{-1}. The amount of carbon formations on the surface of catalysts were determined by measuring the CO and CO_2 yields from the TPO results (using Microcal Origin Software) assuming a value of 0.026 nm^2 for the area occupied by a carbon atom in a surface monolayer of the basal plane in graphite [17].

In order to study the steam reforming reactivity, the rate of hydrocarbon reforming was defined in terms of conversion and product distribution. The yield of hydrogen production was calculated by the hydrogen balance, defined as the molar fraction of hydrogen produced to the total hydrogen in the products. Distributions of other by-products (i.e. carbon monoxide, carbon dioxide, methane, ethane, ethylene, and acetaldehyde for ethanol steam reforming) were calculated by the carbon balance, defined as the ratios of the product moles to the consumed moles of hydrocarbon, accounting for stoichiometry. This information was presented in term of (relative) fraction of all by-product components (i.e. carbon monoxide, carbon dioxide, methane, ethane, and ethylene), which are summed to 100%.

3. Results and discussion

3.1. Steam reforming over Ni/YSZ

Ni/YSZ was tested for the steam reforming of methane, methanol, and ethanol at 900 °C with the inlet fuel/steam molar ratio of 1.0/3.0 (partial pressure of inlet feed of 4 kPa). The reforming rate was measured as a function of time in order to

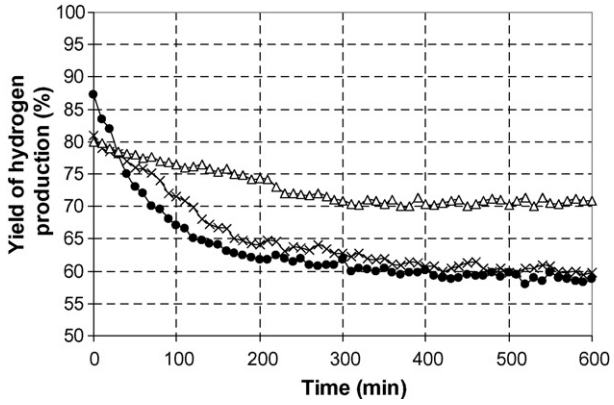

Fig. 2. Yield of H_2 production from the steam reforming of ethanol (●), methanol (×), and methane (△) over Ni/YSZ at 900 °C.

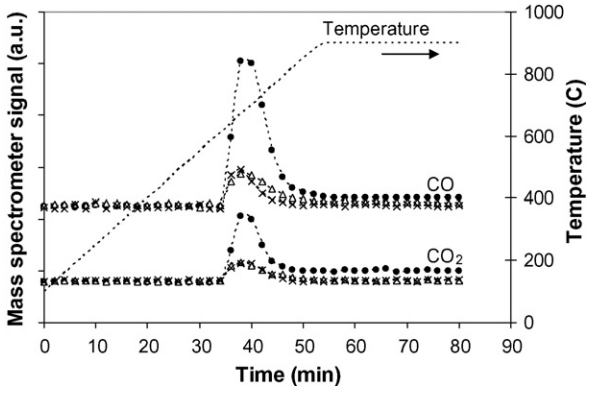

Fig. 3. Temperature-programmed oxidation (TPO) of Ni/YSZ after exposure in steam reforming of ethanol (●), methanol (×), and methane (△) for 10 h.

indicate the stability and the deactivation rate. The variations in the yield of hydrogen production with time at 900 °C are shown in Fig. 2. Significant deactivations were detected from the steam reforming of ethanol and methanol, whereas much lower deactivation was observed from the steam reforming of methane. Catalyst stabilities expressed as deactivation percentages as well as the product distributions from the steam reforming over these fuels are given in Table 2. It is clear that hydrogen, carbon monoxide, and carbon dioxide are the main products from the methane steam reforming. In the cases of methanol and ethanol, methane is also produced along with hydrogen, carbon monoxide, and carbon dioxide. In addition, significant amount of ethane and ethylene are also observed from the steam reforming of ethanol. It should be noted that the thermodynamic analysis of these reactions at 900 °C were also performed using MATLAB program. At equilibrium condition, the main products from these three reactions are only hydrogen, carbon monoxide, and carbon dioxide. Very few amount of methane (2.8×10^{-4} kPa) was detected from the steam reforming of ethanol, whereas no formation of ethane and ethylene was observed from the calculation. These calculated values are also presented in Table 2 (in the blanket). The deviation of the experimental results from the thermodynamic values particularly for the steam reforming of ethanol (i.e. significant formations of methane, ethane, and ethylene), which have also been observed by several researchers [11,18–20], are due to several side reactions. For instance, ethane and ethylene can be formed by the dehydration of ethanol (Eq. (1)) following with the production of ethane by ethylene hydrogenation (Eq. (2)). Simultaneously, methane can be formed by the decomposition and reforming of these ethane and ethylene, methanation [11], and decomposition of ethanol [18].

$$C_2H_5OH \rightarrow C_2H_4 + H_2O \quad (1)$$

$$C_2H_4 + H_2 \rightarrow C_2H_6 \quad (2)$$

According to the catalytic reforming of methanol with steam, the well-known reactions involved in this process can be represented by the decomposition-shift mechanism, Eqs. (3)–(5).

$$CH_3OH = 2H_2 + CO \text{ (methanol decomposition)} \quad (3)$$

$$CO + H_2O = H_2 + CO_2 \text{ (water–gas shift reaction)} \quad (4)$$

$$CO + 3H_2 = CH_4 + H_2O \text{ (methanation)} \quad (5)$$

Firstly, methanol can be directly converted to hydrogen and carbon monoxide by the decomposition process (Eq. (3)). In the presence of steam, the water–gas shift reaction (Eq. (4)) takes place to produce carbon dioxide and more hydrogen. Methane can be formed by the methanation reaction (Eq. (5)). It should be noted that the formations of higher molecular weight compounds such as formaldehyde, methyl formate and formic acid were not observed from the reaction. This observation is in good agreement with the previous work from Lwin et al. [21].

In order to determine the reason of the deactivation in Fig. 2, the post-reaction temperature-programmed oxidation experiments were carried out to investigate the amount of carbon formation on the surface of Ni/YSZ. From the TPO results as shown in Fig. 3, the huge amounts of carbon deposition were observed from the steam reforming of ethanol, whereas much lower carbon formations were detected from the steam reforming of methane. The values of carbon formations (monolayer)

Table 2
Product analysis after exposure in the steam reforming conditions at 900 °C for 10 h

Type of fuel	Deactivation (%)	Yield of H_2 production (%)	Fraction of the by-products (%)				
			CO	CO_2	CH_4	C_2H_6	C_2H_4
Methane	11.3	70.9	68.1[a] (71.7)[b]	31.9 (28.3)	–	–	–
Methanol	26.2	59.7	62.9 (55.0)	27.7 (45.0)	9.4 (∼0)	–	–
Ethanol	32.7	58.3	44.5 (78.2)	11.8 (21.7)	30.2 (∼0)	4.7 (0)	8.8 (0)

[a] Observed from the experiments.
[b] Calculated from the thermodynamic analysis (at equilibrium).

Table 3
Physicochemical properties of the catalysts after reactions

Condition	Ni-load (wt%)	Ni-reducibility (Ni%)
Fresh catalyst	39	95.9
Spent catalyst after exposure in		
Methane steam reforming	38.8	95.5
Methanol steam reforming	39	82.9
Ethanol steam reforming	38.6	92.7

on the surface of catalysts were determined by measuring these CO and CO_2 yields (using Microcal Origin Software). Using a value of 0.026 nm^2 for the area occupied by a carbon atom in a surface monolayer of the basal plane in graphite [17], the quantities of carbon deposited for each inlet fuel (i.e. methane, methanol, and ethanol) were observed to be 0.21, 0.37, and 4.29 monolayer, respectively.

The formations of ethylene and ethane are the major reason for the high rate of carbon formation from the ethanol steam reforming as these components act as very strong promoters for carbon formation [15]. Eqs. (6)–(11) present the most probable reactions that could lead to carbon deposition from the system of the steam reforming of ethanol [15]:

$$C_2H_6 \Leftrightarrow 3H_2 + 2C \quad (6)$$

$$C_2H_4 \Leftrightarrow 2H_2 + 2C \quad (7)$$

$$CH_4 \Leftrightarrow 2H_2 + C \quad (8)$$

$$2CO \Leftrightarrow CO_2 + C \quad (9)$$

$$CO + H_2 \Leftrightarrow H_2O + C \quad (10)$$

$$CO_2 + 2H_2 \Leftrightarrow 2H_2O + C \quad (11)$$

C is the carbonaceous deposits. At low temperature, Eqs. (10) and (11) are favorable, while Eqs. (6)–(9) are thermodynamically unflavored [21]. The Boudouard reaction (Eq. (9)) and the decomposition of hydrocarbons (Eqs. (6)–(8)) are the major pathways for carbon formation at such a high temperature as they show the largest change in Gibbs energy [22]. According to the range of temperature in this study, carbon formation would be formed via the decomposition of hydrocarbons and Boudouard reactions.

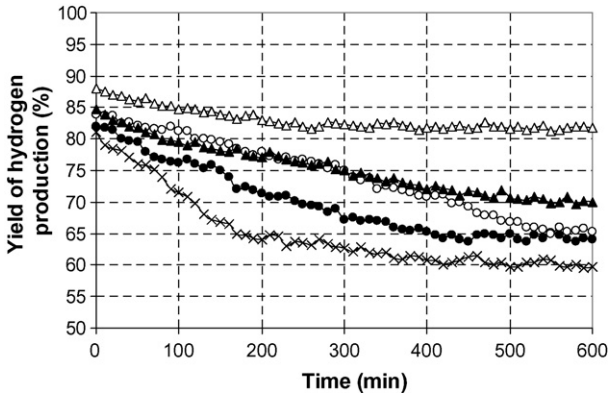

Fig. 4. Yield of H_2 production from the steam reforming of methanol over Ni/YSZ at 900 °C (×), 925 °C (●), 950 °C (◯), 975 °C (▲), and 1000 °C (△).

For the steam reforming of methanol and methane, ethane and ethylene do not appear in the reaction products, the potential formation of carbon species on the surface of catalyst arises from the decomposition and Boudouard reactions. Apart from the carbon formation problem, another major cause for the deactivation from methanol steam reforming is due to the oxidation of Ni, as the reducibility of Ni reduced to 82.9% after exposure in the steam reforming conditions for 10 h, regarding to the TPR experiments (Table 3). It should be noted that the oxidation of Ni/YSZ also occurred after exposure in the ethanol steam reforming conditions.

3.2. *Effects of temperature and fuel/steam ratio on the steam reforming over Ni/YSZ*

The influences of operating temperature and the inlet steam content on the amount of carbon formation and product distribution from the steam reforming of these hydrocarbons were studied by varying temperature from 900 to 1000 °C for three different inlet fuel/steam molar ratios (1.0/3.0, 1.0/4.0, and 1.0/5.0). Fig. 4 shows the effect of temperature on the yield of hydrogen production from methanol steam reforming over Ni/YSZ anode, while Tables 4 and 5 summarize the influences of the inlet steam

Table 4
Products and amount of carbon deposition after exposure in the steam reforming at different inlet fuel/H_2O ratios at 900 °C

Type of fuel	Fuel/H_2O ratio	Yield of H_2 production (%)	Fraction of the by-products (%)					C formation (monolayers)
			CO	CO_2	CH_4	C_2H_6	C_2H_4	
Methane	1.0/3.0	70.9	68.1	31.9	–	–	–	0.21
	1.0/4.0	73.7	65.2	34.8	–	–	–	0.15
	1.0/5.0	77.5	59.3	40.7	–	–	–	0.09
Methanol	1.0/3.0	59.7	62.9	27.7	9.4	–	–	0.37
	1.0/4.0	64.2	60.4	30.5	9.1	–	–	0.32
	1.0/5.0	66.3	57.5	33.8	8.7	–	–	0.26
Ethanol	1.0/3.0	58.3	44.5	11.8	30.2	4.7	8.8	4.29
	1.0/4.0	60.0	42.9	14.9	29.8	4.3	8.1	4.18
	1.0/5.0	61.4	41.2	18.3	29.1	3.9	7.5	4.12

Table 5
Products and amount of carbon deposition after exposure in the steam reforming at different temperatures (inlet fuel/H_2O ratio of 1.0/3.0)

Type of fuel	Temperature (°C)	Yield of H_2 production (%)	Fraction of the by-products (%)					C formation (monolayers)
			CO	CO_2	CH_4	C_2H_6	C_2H_4	
Methane	900	70.9	68.1	31.9	–	–	–	0.21
	925	75.7	71.2	28.8	–	–	–	0.14
	950	78.3	74.0	26.0	–	–	–	0.08
	975	81.6	76.5	23.5	–	–	–	~0
	1000	84.9	79.7	20.3	–	–	–	~0
Methanol	900	59.7	62.9	27.7	9.4	–	–	0.37
	925	64.0	66.7	26.0	7.3	–	–	0.19
	950	65.3	70.3	25.0	4.7	–	–	0.12
	975	70.1	73.4	24.5	2.1	–	–	0.05
	1000	81.8	77.0	22.7	0.3	–	–	~0
Ethanol	900	58.3	44.5	11.8	30.2	4.7	8.8	4.29
	925	60.7	48.9	5.9	32.4	3.5	9.3	4.17
	950	62.9	51.2	5.1	31.7	2.9	9.1	3.94
	975	65.0	53.7	5.0	30.8	1.8	8.7	3.91
	1000	67.2	55.1	6.0	29.5	1.1	8.3	3.82

content and temperature on all product distribution and amount of carbon formation.

Clearly, the amount of carbon formation from the steam reforming of methanol and methane significantly decreased with increasing temperature and inlet steam concentration. These are due to the higher reforming reactivity of methane and methanol at high temperature and inlet steam concentration. In addition, it was also observed that the oxidized state of Ni/YSZ from the steam reforming of methanol and ethanol decreased with increasing temperature. In contrast, the amount of carbon formation from the steam reforming of ethanol slightly changed with increasing temperature and inlet steam concentration. Although the formations of ethane, and ethylene from the steam reforming of ethanol decreased with increasing temperature and inlet steam concentration, significant amount of these hydrocarbons remain observed even at the temperature as high as 1000 °C (Table 5).

Considering product distribution from the steam reforming, the yield of hydrogen production and carbon monoxide fraction increased with increasing temperature, whereas carbon dioxide and methane production fraction decreased. Regarding the effect of steam, hydrogen and carbon dioxide fraction increased with increasing inlet steam concentration, whereas carbon monoxide fraction decreased. The yield of methane production reduced at higher temperature. It should be noted that the changes of hydrogen, carbon monoxide, and carbon dioxide are mainly due to the influence of mildly exothermic water–gas shift reaction ($CO + H_2O \rightarrow CO_2 + H_2$), whereas the decrease of methane production is due to the further reforming to carbon monoxide and hydrogen.

3.3. Steam reforming with IIR-SOFC configuration

It is clear from the above observation that ethanol cannot be used as the inlet fuel for DIR-SOFC operation due to the easy degradation of Ni/YSZ anode. In contrast, methane with high steam content can be directly fed to Ni/YSZ anode, while methanol could also be used as the direct feed at a temperature as high as 1000 °C. The next approach is to investigate the possible uses of ethanol and methanol at lower operating temperature in IIR-SOFC operation by performing the reaction in the annular ceramic reactor as described above.

With the same feeding conditions, Fig. 5 shows the variations in the yield of hydrogen production with time at 900 °C over this configuration compared to those from the system with only Ni/YSZ. The yields of hydrogen production from the steam reforming of all hydrocarbon feeds over this configuration were considerably higher than those of single Ni/YSZ. In addition, according to the TPO after reaction, the amounts of carbon formation on the surface of Ni/YSZ were significantly reduced (Table 6). These improvements are due to the conversion of all alcohol and high hydrocarbon components from the decomposition of ethanol (i.e. ethylene and ethane) to methane, carbon monoxide, and hydrogen by Ni/Ce–ZrO_2 before these components reach the surface of Ni/YSZ at the outer side of the annular reactor. Therefore, the main reaction on the surface of Ni/YSZ is the steam reforming of methane, which is thermodynamically unflavored to form carbon deposition, instead of the steam reforming of alcohol or high hydrocarbon.

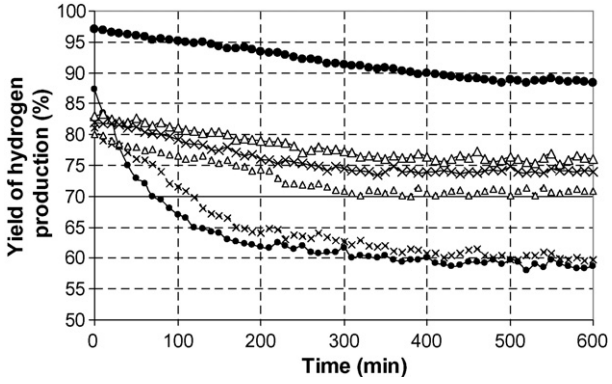

Fig. 5. Yield of H_2 production from the steam reforming of ethanol (●), methanol (×), and methane (△) over Ni/Ce–ZrO_2 + Ni/YSZ at 900 °C compared to those over Ni/YSZ in Fig. 2 (dot line with small symbols).

Table 6
Products and amount of carbon deposition from the steam reforming over Ni/Ce–ZrO_2 + Ni/YSZ at different temperatures (inlet fuel/H_2O ratio of 1.0/3.0)

Type of fuel	Temperature (°C)	Yield of H_2 production (%)	Fraction of the by-products (%)					C formation (monolayers)
			CO	CO_2	CH_4	C_2H_6	C_2H_4	
Methane	700	55.3	58.2	41.8	–	–	–	0.09
	750	60.0	60.7	39.3	–	–	–	~0
	800	67.6	64.4	35.6	–	–	–	~0
	850	72.9	69.0	31.0	–	–	–	~0
	900	76.1	72.1	27.9	–	–	–	~0
Methanol	700	51.0	51.0	45.2	3.8	–	–	0.13
	750	58.6	53.8	44.1	2.1	–	–	0.05
	800	64.1	57.9	40.6	1.5	–	–	~0
	850	69.9	60.5	38.8	0.7	–	–	~0
	900	73.9	64.1	35.9	–	–	–	~0
Ethanol	700	67.9	37.1	18.8	22.0	12.6	9.5	3.97
	750	71.6	40.2	16.5	34.7	6.7	1.9	2.83
	800	75.9	47.9	15.0	34.2	2.9	~0	2.39
	850	81.2	55.6	12.7	31.7	~0	~0	0.66
	900	88.4	61.3	11.9	26.8	~0	~0	0.42

The effect of temperature on the degree of carbon formation over Ni/YSZ was then studied by varying the operating temperature from 700 to 900 °C. As also seen in Table 6, methanol can be used as the feed in all range of this temperature with only small amount of carbon deposition detected on the surface of Ni/YSZ at low temperature. In contrast, at the temperature of 700–800 °C, the amount of carbon deposition on the surface of Ni/YSZ when ethanol was used as the feed is considerably high, but it decreases significantly when the temperature is higher than 900 °C. The high carbon formation could be due to the incomplete reforming of ethanol, ethane, and ethylene at the temperature lower than 900 °C. Fig. 6 shows the effect of temperature on the ethanol conversion and product distribution from the ethanol steam reforming over Ni/Ce–ZrO_2. It is clear from the figure that all ethanol, ethane, and ethylene are reformed at the temperature above 850 °C.

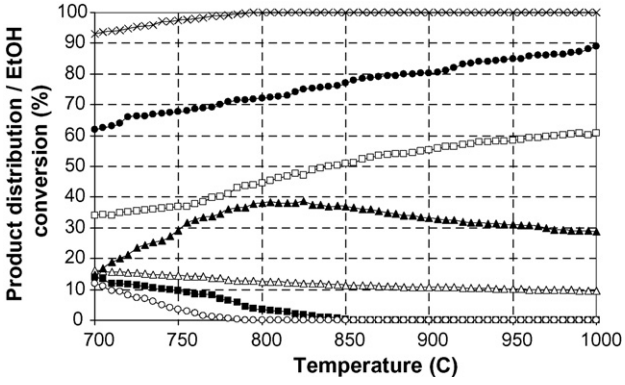

Fig. 6. Effect of temperature on the conversion of EtOH (×), the fractions of CO (□), CO_2 (△), CH_4 (▲), C_2H_6 (◯), and C_2H_4 (■), and the yield of H_2 production (●) from ethanol steam reforming over Ni/Ce–ZrO_2 (4 kPa EtOH and 12 kPa H_2O).

3.4. Steam reforming of methanol over Ni/YSZ with preliminary homogeneous reforming

From the above observation, methanol with steam can be directly fed to the anode side of fuel cell (DIR) at such a high temperature, 1000 °C, without the problem of carbon formation. In contrast, when fuel cell is operated at lower temperature (700–975 °C), methanol must be firstly converted to methane and other small molecular weight products in the catalytic reformer (IIR).

Nevertheless, it has been reported in the previous publication [23] that methanol can homogeneously decompose to CH_4,

Table 7
Effect of temperature on the homogeneous (in the absence of catalyst) reactivity of methanol steam reforming (1 kPa MeOH and 3 kPa steam)

Temperature (°C)	Methanol conversion (%)	Yield of H_2 production (%)	Fraction of the by-products (%)		
			CO	CO_2	CH_4
800	0.8	0.2	0.5	0.1	0.2
825	4.1	0.8	2.1	1.0	1.3
850	16.5	6.1	10.0	2.4	4.0
875	52.1	12.3	27.6	3.7	20.8
900	93.2	20.9	46.3	7.3	39.5
925	~100	23.3	50.2	8.6	41.2
950	~100	23.7	50.1	8.3	41.6
975	~100	23.4	50.1	8.4	41.5
1000	~100	23.5	50.1	8.0	41.8

Table 8
Products and amount of carbon deposition after exposure in methanol steam reforming over Ni/YSZ with preliminary homogeneous reforming

Temperature (°C)	Deactivation (%)	Yield of H_2 production (%)	Fraction of the by-products (%)			C formation (monolayers)
			CO	CO_2	CH_4	
900	11.9	70.8	65.7	31.6	2.7	0.18
925	21.8	72.3	68.2	29.9	1.9	0.11
950	22.1	74.9	74.3	25.7	~0	~0
975	17.3	79.6	75.1	24.9	~0	~0
1000	7.1	83.9	79.9	20.1	~0	~0

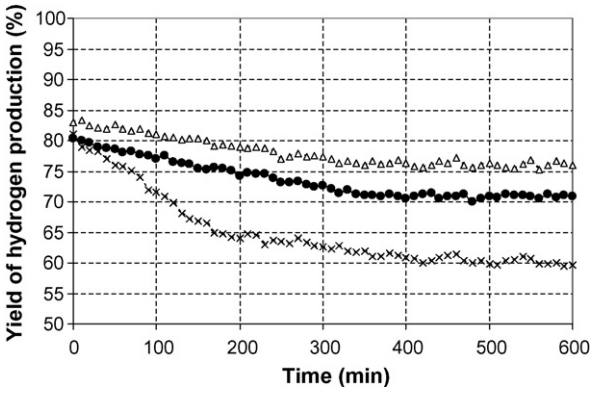

Fig. 7. Yield of H_2 production from methanol steam reforming over Ni/YSZ with preliminary homogeneous reforming at 900 °C (●) compared to that without homogeneous reforming in Fig. 2 (×) and that over Ni/Ce–ZrO_2 + Ni/YSZ in Fig. 5 (△).

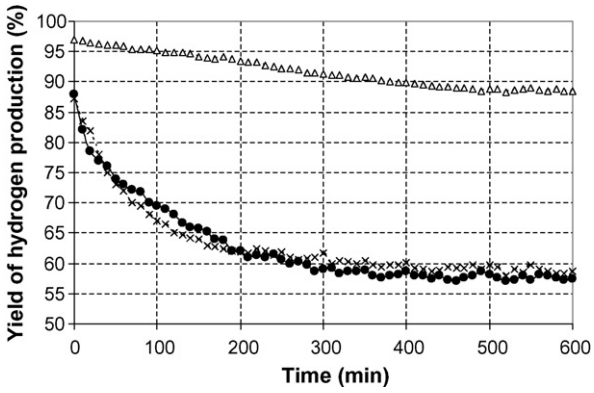

Fig. 8. Yield of H_2 production from ethanol steam reforming over Ni/YSZ with preliminary homogeneous reforming at 900 °C (●) compared to that without homogeneous reforming in Fig. 2 (×) and that over Ni/Ce–ZrO_2 + Ni/YSZ in Fig. 5 (△).

CO, CO_2, and H_2 at high temperature. Therefore, this benefit was also considered in this work. Firstly, the homogeneous (non-catalytic) decomposition of methanol was investigated by feeding CH_3OH/H_2O in helium to the blank reactor and the temperature was increased from 200 to 1000 °C. It was observed that methanol was converted to methane, carbon monoxide, carbon dioxide, and hydrogen at the temperature above 800 °C (Table 7). These components were formed via the decomposition of methanol, water–gas shift, and methanation reactions.

The annular ceramic reactor was then applied without the filling of Ni/Ce–ZrO_2 at the inner side of the tube; only Ni/YSZ was packed at the outer side. Methanol and steam were fed through the inner side of the annular reactor before flowing backward through the outer side where catalytic steam reforming took place. Fig. 7 and Table 8 present the stability, product distribution, and degree of carbon deposition (from TPO testing) from this system. Surprisingly, the amount of carbon formation on the surface of Ni/YSZ decreases considerably when the operating temperature is higher than 900 °C. In addition, the catalyst stability and hydrogen yield increase significantly.

The improvements are due to the homogeneous cracking of methanol to CH_4, CO, CO_2, and H_2 before reaching the surface of Ni/YSZ. At the temperature higher than 900 °C, the conversion of methanol is closed to 100%, therefore, the main reaction at the surface of Ni/YSZ is the steam reforming of methane, which is thermodynamically unflavored to form carbon deposition compared to the steam reforming of methanol.

For comparison, the steam reforming of ethanol over Ni/YSZ with preliminary homogeneous reforming was also studied. Similar to the methanol case, the homogeneous (non-catalytic)

Table 9
Effect of temperature on the homogeneous (in the absence of catalyst) reactivity of ethanol steam reforming (1 kPa EtOH and 3 kPa steam)

Temperature (°C)	Yield of H_2 production (%)	Fraction of the by-products (%)					
		CH_3CHO	CO	CO_2	CH_4	C_2H_6	C_2H_4
200	~0	1.3	0	0	0	0	0
300	11.9	21.1	5.1	0	0.5	0	0
400	23.2	31.9	10.9	3.2	3.1	0	0
500	31.4	37.4	16.2	7.8	5.3	0	0
600	37.8	24.8	21.5	9.4	5.5	16.1	8.1
700	43.0	0	29.2	9.7	5.9	23.9	19.2
800	46.2	0	29.1	9.6	5.8	23.4	19.8
900	48.5	0	29.3	9.4	6.0	22.2	20.0
1000	49.8	0	28.9	9.6	5.9	22.3	19.8

Table 10
Products and amount of carbon deposition after exposure in ethanol steam reforming over Ni/YSZ with preliminary homogeneous reforming

Temperature (°C)	Deactivation (%)	Yield of H_2 production (%)	Fraction of the by-products (%)					C formation (monolayers)
			CO	CO_2	CH_4	C_2H_6	C_2H_4	
900	34.7	57.4	46.7	10.5	31.6	5.1	6.1	4.38
950	31.9	61.9	54.7	5.3	31.9	3.2	4.9	3.86
1000	28.4	68.6	59.2	5.8	30.2	1.4	3.4	3.84

steam reforming of ethanol was primarily investigated. The inlet C_2H_5OH/H_2O in helium with the molar ratio of 1.0/3.0 (inlet C_2H_5OH of 4 kPa) was introduced to the blank reactor, while the temperature increased from 200 to 1000 °C. As presented in Table 9, it was observed that ethanol was converted to acetaldehyde, and hydrogen at the temperature above 200 °C. Methane and carbon monoxide productions were then observed from the decomposition of acetaldehyde at the temperature of 250–300 °C. When the temperature increased up to 550 °C, the selectivity of acetaldehyde significantly decreased, while hydrogen, carbon monoxide, and carbon dioxide remained increasing. At the temperature above 550 °C, the formations of ethane and ethylene were also observed due to the dehydration of ethanol following with the production of ethane by ethylene hydrogenation.

The annular ceramic reactor was then applied by feeding ethanol and steam through the blank inner side of the annular reactor before flowing backward through the outer side where Ni/YSZ was filled. Significant deactivation was detected from this system (Fig. 8). In addition, high amount of carbon formation was observed on the surface of Ni/YSZ in all ranges of temperature, according to the TPO testing (Table 10). This is due to the presents of ethylene and ethane, which are very strong promoters for carbon formation. Therefore, it is clear that ethanol cannot be fed directly to Ni/YSZ even with the preliminary homogeneous reforming.

4. Conclusion

Methane with high steam content can be directly fed to Ni/YSZ anode without the problem of carbon formation, while methanol can be used as the direct feed at the temperature as high as 1000 °C. In contrast, ethanol cannot be used as the direct fuel for DIR-SOFC operation (with Ni/YSZ anode) even at high steam content and high operating temperature due to the easy degradation of anode material; it must be first converted to methane by the catalytic reformer (IIR-SOFC operation). Ni/Ce–ZrO_2 was found to be a good internal reforming catalyst in the present work.

It was then found from the study that methanol can be efficiently fed to Ni/YSZ anode (as DIR operation) at lower temperature (900–975 °C) without the problem of carbon formation if SOFC system has sufficient space volume at the entrance of the anode chamber where methanol is homogeneously converted to CH_4, CO, CO_2, and H_2 before reaching SOFC anode.

Acknowledgements

The financial support from The Thailand Research Fund (TRF) throughout this project is gratefully acknowledged. The authors would also like to express gratitude to Mr. Pakorn Philunrekekun for the thermodynamic analysis.

References

[1] N.Q. Minh, T. Takahashi, Science and Technology of Ceramic Fuel Cells, Elsevier, Amsterdam, 1995.
[2] W.L. Lundberg, S.E. Veyo, in: Yokohawa, S.C. Singhal (Eds.), Proceeding of the 7th International Symposium Solid Oxide Fuel Cells VII, 2001, p. 78.
[3] S.H. Clarke, A.L. Dicks, K. Pointon, T.A. Smith, A. Swann, Catal. Today 38 (4) (1997) 411.
[4] K.C. Wincewicz, J.S. Cooper, J. Power Sources 140 (2005) 280.
[5] I.V. Yentekakis, S.G. Neophytides, A.C. Kaloyiannis, C.G. Vayenas, Proceeding of the 3rd International Symposium on Solid Oxide Fuel Cells, vol. 4, Honolulu, HI, USA, 1993, p. 904.
[6] E. Achenbach, E. Riensche, J. Power Sources 52 (1994) 283.
[7] A.L. Dicks, K.D. Pointon, A. Siddle, J. Power Sources 86 (2000) 523.
[8] B. Emonts, J.B. Hansen, S.L. Jorgensen, B. Hohlein, R. Peters, J. Power Sources 71 (1998) 288.
[9] K. Ledjeff-Hey, V. Formanski, T. Kalk, J. Roes, J. Power Sources 71 (1–2) (1998) 199.
[10] S. Cavallaro, S. Freni, Int. J. Hydrogen Energy 21 (6) (1996) 465.
[11] A.N. Fatsikostas, X.E. Verykios, J. Catal. 225 (4) (2004) 439.
[12] S.L. Douvartzides, F.A. Coutelieris, K. Demin, P.E. Tsiakaras, AIChE J. 49 (2003) 248.
[13] N. Laosiripojana, S. Assabumrungrat, Appl. Catal. A 290 (2005) 200.
[14] N. Laosiripojana, S. Assabumrungrat, J. Power Sources 158 (2) (2006) 1348.
[15] N. Laosiripojana, S. Assabumrungrat, Appl. Catal. B 66 (1–2) (2006) 29.
[16] N. Laosiripojana, S. Assabumrungrat, Appl. Catal. B 60 (2005) 107.
[17] E. Ramirez, A. Atkinson, D. Chadwick, Appl. Catal. B 36 (2002) 193.
[18] F. Aupretre, C. Descorme, D. Duprez, D. Casanave, D. Uzio, J. Catal. 233 (2) (2005) 464.
[19] J. Comas, F. Mariño, M. Laborde, N. Amadeo, Chem. Eng. J. 98 (1–2) (2004) 61.
[20] M.A. Goula, S.K. Kontou, P.E. Tsiakaras, Appl. Catal. B 49 (2) (2004) 135.
[21] Y. Lwin, W.R.W. Daud, A.B. Mohamad, Z. Yaakob, Int. J. Hydrogen Energy 25 (1) (2000) 47.
[22] J.N. Armor, Appl. Catal. A: Gen. 176 (1999) 159.
[23] N. Laosiripojana, S. Assabumrungrat, Chem. Eng. Sci. 61 (8) (2006) 2540.